applied sciences

MDPI

Article

Process Monitoring Using Kernel PCA and Kernel Density Estimation-Based SSGLR Method for Nonlinear Fault Detection

Faisal Shahzad [1], Zhensheng Huang [1,*] and Waqar Hussain Memon [2]

[1] Department of Statistics and Financial Mathematics, School of Sciences, Nanjing University of Science and Technology, Nanjing 210094, China; faisalshahzad@njust.edu.cn
[2] Department of Mechanical Engineering, School of Sciences, Nanjing University of Science and Technology, Nanjing 210094, China; waqarmemon@njust.edu.cn
* Correspondence: zshuang@njust.edu.cn

Abstract: Fault monitoring is often employed for the secure functioning of industrial systems. To assess performance and enhance product quality, statistical process control (SPC) charts such as Shewhart, CUSUM, and EWMA statistics have historically been utilized. When implemented to multivariate procedures, unfortunately, such univariate control charts demonstrate low fault sensing ability. Due to some limitations of univariate charts, numerous process monitoring techniques dependent on multivariate statistical approaches such as principal component analysis (PCA) and partial least squares (PLS) have been designed. Yet, in some challenging scenarios in industrial chemical and biological processes with notably nonlinear properties, PCA works poorly, according to its presumption that the dataset generally be linear. However, Kernel Principal Component Analysis (KPCA) is a reliable and precise nonlinear process control methodology, but the interaction mainly through upper control limits (UCLs) dependent on the Gaussian distribution may weaken its output. This article introduces time-varying statistical error tracking through Kernel Principal Component Analysis (KPCA) based on Generalized Likelihood Ratio statistics (GLR) using a sequential sampling scheme named KPCA-SSGLR for nonlinear fault detection. The main issue of employing just T^2 and Q statistic in KPCA is that they cannot correctly give practitioners the change point of the system fault, preventing practitioners from diagnosing the issue. Based on this perspective, this study attempts to incorporate KPCA with sequential sampling Generalized Likelihood Ratio (SSGLR) for monitoring the nonlinear fault in multivariate systems. The KPCA is utilized for dimension reduction, while the SSGLR is employed as a tracking statistic. The kernel density estimation (KDE) was employed to approximate UCLs for variational system operation relying on KPCA. The testing efficiency of the corresponding KPCA-KDE-SSGLR technique was then analyzed and competed with KPCA and kernel locality preserving projection (KLPP), the UCLs of which were focused on the Gaussian distribution. The purpose of this analysis is to enhance the development of KPCA-KDE-SSGLR to accomplish future enhancements and to advance the practical use of the established model by implementing the sequential sampling GLR approach. The fault monitoring efficiency is demonstrated through different simulation scenarios, one utilizing synthetic data, the other from the Tennessee Eastman technique, and lastly through a hot strip mill. The findings indicate the applicability of the KPCA-KDE-based SSGLR system over the KLPP and KPCA-KDE methods by its two T^2 and Q charts to recognize the faults.

Keywords: generalized likelihood ratio chart; multivariate statistics; kernel principal component analysis; kernel density estimation; fault detection and identification; kernel locality preserving projections

Citation: Shahzad, F.; Huang, Z.; Memon, W.H. Process Monitoring Using Kernel PCA and Kernel Density Estimation-Based SSGLR Method for Nonlinear Fault Detection. *Appl. Sci.* **2022**, *12*, 2981. https://doi.org/10.3390/app12062981

Academic Editors: João Carlos de Oliveira Matias and Paolo Renna

Received: 18 January 2022
Accepted: 11 March 2022
Published: 15 March 2022

1. Introduction

Fault assessment serves a pivotal part in maintaining the consistency of manufacturing as well as factory enrichment. Several factors are monitored in different working units within newly constructed industrial process units, and these factors are captured at several

time periods. The generated data points are strongly linked and contain a significant amount of distortion. Relatively very less information can be retrieved in the absence of an adequate mechanism for analyzing relevant inputs, and as a result, maintenance crews have an inadequate grasp of the mechanism. Because of this misunderstanding, the operation becomes unsteady. Statistical process control (SPC) provides the most potent mechanism for detecting imperfection scope. Control charts are widely employed to describe modifications in systems that can react to a degradation of the commodity's output and track the function of industrial output. Statistical process control (SPC) charts, notably Shewhart, CUSUM, and EWMA, have been applied to analyze procedures and enrich product performance in the previous era. Consequently, experiments have demonstrated that these approaches are ineffective in identifying significant variations in the system. Establishing a valuable detection framework for identifying means shifts is becoming a critical problem in a simple operation.

A few of the drawbacks of a univariate control system are that specific parameters can indeed be measured and manipulated for a singular process [1]. This provokes the elaboration of multivariate quality control approaches to address these drawbacks by testing multiple factors simultaneously [2]. Through multivariate methodology, professionals and manufacturing firms that track complicated systems can regulate their system's reliability. The kernel principal component analysis (KPCA) has become one of the increasingly prevalent nonlinear statistical techniques [3]. Statistical flaw detection methods focused on hypothesis tests, such as the Generalized Likelihood Ratio chart (GLR), seem useful calculation statistics for PCA and KPCA. The Generalized Likelihood Ratio (GLR) framework is a statistical hypothesis method that utilizes the principle of maximum likelihood estimation. Therefore, it is designed to have the optimal identification outcomes as it significantly increases the detection accuracy with a specific false warning rate [4]. It is one of the leading efficient strategies of univariate system identification. The GLR framework presently used throughout research (attributed to residues derived from the PCA concept) was developed to monitor the mean changes for numerous purposes, including ozone research [5] and chemical process data [6].

The foremost aim of this article is to analyze the sequential sampling GLR chart's efficiency under multiple fault situations through a nonlinear system identification algorithm that relies on KPCA-KDE. With such a short measurement of the SPE in future space, the KDE framework is used to generate UCLs for PCA and KPCA. In a linear approach such as PCA, the estimation of the upper control limits (UCLs) is dependent on the proposition that the state variables used in the measurements are Gaussian. Based on this statement, the specific model can be extracted analytically. The UCLs can therefore also be extracted analytically.

Moreover, numerous actual manufacturing systems are nonlinear. Although the origin of such a system's unpredictability may be considered Gaussian, the variables used in the calculated results are non-Gaussian due to the intrinsic nonlinearities. Thus, the adoption of UCLs for fault diagnosis depending on multivariate Gaussian assumptions in such methods is improper, in addition to that it can contribute to imprecise outcomes.

Current GLR charts research assesses the output utilizing ARL_1 measurements [4,7,8]. The next importance of this study is to investigate the SSGLR chart's efficiency using all necessary fault diagnosis conditions: false detection rate (FDR), false alarm rate (FAR), and ARL_1. Ref. [9] implemented a linear PCA-based GLR to identify faults, such that the dataset will be first designed using a linear PCA framework. Afterward, the flaws are identified through GLR statistics. The drawback of PCA is that it is not applicable in nonlinear situations and suggests that the interaction amongst variables is linear, thus might not necessarily be the most acceptable measurement form.

In conclusion, several chemical mechanisms, such as fractional distillation, are typically represented as nonlinear systems. Numerous measures have been developed [10] (Choi et al., [11] and Nguyen and Sheriff et al. [12]) to fix nonlinear PCA extensions and to produce virtuous results across linear models. KPCA is amongst the most renowned

nonlinear mathematical techniques [11] (Schoellkopf et al. (1997) [3], Hoffmann [13], and Fan et al. [14]) which is a tool for performing a nonlinear type of principal component analysis that can effectively measure main components in elevated structures linked to input space through specific nonlinear modeling and assessment. As a result, in this study, we tackle the problem of nonlinear fault identification by first modeling the data with the KPCA method and then detecting the faults with SSGLR. In reality, the KPCA model has proved to be effective in obtaining realistic principal components of a collection of the data and dealing with variable nonlinearity. By reflecting the source data onto a space with much fewer dimensions, the KPCA model reduces the complexity of the data. The KPCA is employed to build the model and discover nonlinear combinations of parameters that characterize the significant patterns in a dataset, while the SSGLR is employed to find flaws. Both are used to enhance the flaw detection method.

The rest of the article is designed as follows. In Section 2, an overview of the KPCA-KDE procedure is provided, accompanied by an explanation of the two primary identification metrics, T^2 and Q, which are typically utilized with the KPCA for fault identification. The Generalized Likelihood Ratio (GLR) statistics using a sequential sampling scheme developed to identify faults are then discussed in Section 3. Section 4 sets out the KPCA-KDE-based SSGLR method of analysis and highlights how it can be applied to monitor online procedures. Section 5 provides an illustration of synthetic data assessing the efficacy of KPCA-KDE-SSGLR statistics under specific fault situations. Section 6 is designed to analyze and compare the effectiveness of KPCA-KDE-SSGLR and KLPP. Implementation of tracking initiatives to the TE benchmarking method is described in Section 7. Lastly, the conclusions grasped from the research are stated in Section 8.

Literature Review

Synthetic nonlinear data can be simulated through the following. In 1924, Shewhart [15] initially introduced an $\overline{X}$-chart to track output metrics online in an attempt to identify deficiencies in the system in the right direction. However, only recent observations were taken into account in the $\overline{X}$-chart. Hence, it is inefficient to identify minor and medium mean changes in the procedure. The Cumulative Sum (CUSUM) defined by Page [16] and the Exponentially Weighted Moving Average (EWMA) suggested by Roberts [17] take into consideration previous results to detect slight mean changes in the procedure. As a result, investigations have shown that both techniques are inadequate at detecting substantial system alterations. This prompts the development of multivariate quality control systems to solve these flaws by concurrently assessing numerous aspects [2]. Experts and industrial organizations that monitor complex processes can control their system's dependability using the multivariate approach. Chi-square and Hotelling T^2 charts [18] are the most prominent multivariate control charts. In particular, these models are an expansion of the univariate Shewhart-type control chart. Thus, they are generally prone to minor and medium system changes.

Healy [19] suggested a multivariate CUSUM (MCUSUM) monitoring plan resulting through a Sequential Probability Ratio Test (SPRT). The MCUSUM successfully identifies changes all along the pre-specific path defined by the out-of-control mean curve. This indicates that MCUSUM may be unsuccessful if the system requires turning in an unexpected direction. Lowery et al. [20] described a multivariate EWMA (MEWMA) process chart that has been irreducible in the context of the change. Its efficiency has been perceived to be at a minimum as high as MCUSUM. Wang and Reynold [21] further developed a multivariate GLR monitoring model and demonstrated that the MGLR chart may provide significantly superior total efficiency in predicting a considerable variation of changes. The other option of advancing performance is using the GLR (Generalized Likelihood Ratio) control charts based on Sequential Probability Ratio measures. The literature has too many GLR statistic discoveries to track: Bernoulli/binomial models and procedures, GLR charts for geometric observation, auto-correlated structures, and univariate standard processes. For reference,

see Xu et al. [22], Huang et al. [7], Shahzad and Huang [8], Reynolds and Lou [4], Apley and Shi [23], and Lai [24].

There seems to be a growing concern in multivariate statistical process monitoring (MSPM) across both scientific and corporate systems. Specific renowned data-focused fault analysis approaches have been established comprising independent component analysis (ICA) [25], principal component analysis (PCA), partial least squares (PLS) [26,27], and canonical variate analysis (CVA) [28].

PCA-based instability analysis and evaluation is an appealing factual domain and has received substantial interest among numerous researchers in the disciplines (Yoon and MacGregor [29]). PCA (Jackson [30]) is a multivariate statistical process control (MSPC) methodology used to diagnose irregularities in the evaluation of heavily reliant factors. The PCA's central research goal is to quantify observations and factors. It also minimizes the uncertainty of original data (X) by moving data selection to a restricted dataset and compiling specific parameters to protect many current dataset descriptions.

The PCA concept describes a dataset (consisting of many system factors) using a smaller range of preserved variables identified as the key elements representing much of the model uncertainties. This improves computing performance, reducing the time to locate and transmit flaws. These properties make it a prominent option for surveillance of the manufacturing processes (Chiang et al. [31]). Two operational measurements are occasionally employed with the PCA concept; for details, see Sheriff et al. [9]. The Hotelling T^2 metric tracks irregularities in the PCA framework, and the Q statistic evaluates fluctuations in the residual storage provided by the PCA method. Such charts were primarily expended to distinguish changes in variance, mean, and concurrently mean/variance tracking for the control chart.

In addition to that, PCA is a linear strategy and thus would not recognize or identify any nonlinearity involved in several other actual engineering processes [10]. Its output is thus reduced once added to systems that show significant nonlinear component associations. Kramer [32] established a nonlinear PCA approach focused on auto-associative neural networks to solve the variational issue. Consequently, the framework suggested by Kramer is complicated to practice since it has multiple phases. In addition, it would be problematic to calculate the number of neural networks. Dong and McAvoy [33] suggested a nonlinear PCA integrating the critical function and the neural network (NN). Nonlinear PCA approaches have been further suggested by Jia et al., Cheng and Chiu, and Kruger et al. [5,6,34]. However, these kinds of approaches are dependent on NNs, which demand a platform for a nonlinear computation issue.

Scholkopf et al. [35] suggested that the Kernel PCA (KPCA) be a nonlinear extension of the PCA. KPCA could effectively approximate PCs in elevated domains using combined operations, including nonlinear kernel functions. The fundamental concept of KPCA is to first transform the source space to a feature space through variational modeling and afterward calculate the PCs within the feature space. For any procedure that can be represented purely in contexts of dot products (for example, despite the explicit practice of the variables themselves), such kernel approach allows the creation of various nonlinear variants of the existing procedure (Christianini and Shawe-Taylor) [36]. Compared to many nonlinear techniques, the primary benefit of KPCA is that it does not entail nonlinear virtualization (Scholkopf et al. [28]); it involves just linear algebra, rendering it as straightforward as traditional PCA. Like the PCA, the Hotelling T^2 metrics and the Q statistics (as well recognized as squared prediction error, SPE) are two calculation indicators used by the KPCA. The T^2 statement is a measurement of the alteration obtained in the reference frame, and hence the Q factor is employed to track the variability in the residual domain.

2. Kernel Principal Component Analysis (KPCA)

Kernel Principal Components Analysis is a nonlinear PCA extension that comprises observations to a more enormous (potentially infinite) dimensional feature structure using a nonlinear array and then measuring dot products in a feature space. As an approximation

is used in future space, the KPCA is retrieved. KPCA is a kind of kernel-based computing system. KPCA's central premise is, therefore, logical and popular. The fundamental premise of KPCA is to allocate the source values x to the function feature space, first employing a nonlinear projection and afterward implementing a regular PCA in future space.

A dataset matrix was identified by n measurements representing m variables, so that the matrix X is defined as:

$$X = (x_1, x_2, x_3 \dots x_n) = \begin{pmatrix} x_{11} & \cdots & x_{1n} \\ \vdots & \ddots & \vdots \\ x_{m1} & \cdots & x_{mn} \end{pmatrix}$$

The covariance matrix in the domain of a function is then determined as:

$$C_F = 1/n \sum_{i=1}^{n} (\Phi(x_i), \Phi(x_i)) \tag{1}$$

where Φ is the nonlinear mapping due to which the the measured inputs are extended into hyper dimensional feature space and $\Phi(x_i)$ is anticipated to take unit variance and zero mean. To diagonalize the covariance matrix, we illustrate the eigenvalue hitch in the feature space as:

$$\lambda_A = C_F A \tag{2}$$

where λ is an eigenvalue of C_F and A is the consequent eigenvector ($\lambda \geq 0,\ A \neq 0$), where $A = \sum_{j=1}^{n} A_i \langle \Phi(x_j) \rangle$.

The eigenvectors of C_F are specified by:

$$\frac{1}{n} \sum_{j=1}^{n} A_i \langle \Phi(x_k), \sum_{i=1}^{n} \Phi(x_i) \rangle \langle \Phi(x_i), \Phi(x_j) \rangle \tag{3}$$

Rather than conducting eigenvalue reduction explicitly on C_F in Equation (1) and figuring eigenvalue and principal components (PCs), we employ the kernel trick by describing the $n \times n$ (kernel) matrix as follows:

$$[\mathbf{K}]_{ij} = K_{ij} = (\Phi(x_i), \Phi(x_i)) = k(x_i x_j) \tag{4}$$

For all $i, j = 1, 2, \dots, n$, presenting the kernel function of the system $k(x, y) = \langle \phi(x), \phi(y) \rangle$ in Equation (4) allows the computation of the inner products $\langle \phi(x_i), \phi(x_j) \rangle$ in the feature space as a function of the response statistics. This prohibits the necessity to conduct the nonlinear mappings and the explicit computation of inner products in the feature space (Schoellkopf et al., 1998) [35]. Employing the kernel matrix, we revise Equation (4) as $\lambda m \mathbf{K} \alpha = \mathbf{K}^2 \alpha$ for $k = 1, 2, \dots, n$, where it is comparable to the eigenvalue problem as $\lambda m \alpha = \mathbf{K} \alpha$.

The kernel matrix can be mean centered as follows:

$$\mathbf{K}_{ct} = \mathbf{K} - U\mathbf{K} - \mathbf{K}U + U\mathbf{K}U \tag{5}$$

where $\boldsymbol{U}$ is an $n \times n$ matrix in which each integral is equivalent to $\frac{1}{n}$, and $\mathbf{K}$ is the kernel trick. Eigen breakdown of $\mathbf{K}_{ct}$ is identical to the output of PCA in R^F. This totals to determining the eigenvalue problem, which produces eigenvectors $\alpha_1, \alpha_2, \dots \alpha_n$ and the consequent eigenvalues $\lambda_1 \geq \lambda_2 \dots \lambda_n$.

Meanwhile, the kernel matrix $\mathbf{K}_{ct}$ is symmetric, and the resulting principal components are orthonormal, such as:

$$\langle \alpha_i, \alpha_j \rangle = \delta_{i,j} \tag{6}$$

where $\delta_{i,j} = (i, j = 1, 2 \dots m)$ signifies the Dirac delta function.

The score vectors of the nonlinear mapping of mean centered training observations x_j, $i = 1, 2, \dots, n$, can then be obtained by projecting $\phi(x_j)$ onto the principal component space spanned by the eigenvectors α_k, $k = 1, \dots, m$, and applying the kernel

trick, so we can obtain the below equation, and by using this equation we can obtain the nonlinear components.

$$z_{k,j} = \sum_{i=1}^{n} \alpha_{k,i} [\mathbf{K}_{ct}]_{i,j} \quad (7)$$

To determine how many PCs to retain, different procedures may be needed, such as the scree map, the likelihood model [37], cumulative percent variability (CPV), parallel estimation, concurrent checks, re-sampling, and characteristic likelihood (Jolliffe (2002) [38]). CPV is widely used, as it is easy to measure and frequently offers consistent effects. The series of key components to be retained must be persistently centered on the lowest collection of functional variables required to fulfill the CPV. Taking into consideration that 95% of the overall percentage variance (CPV) is sustained:

$$CPV(k) = \frac{\sum_{i=1}^{k} \lambda_i}{trace(\Sigma)} = 0.95 \quad (8)$$

The innovative data matrix can promptly be signified as $X = X\hat{P}\hat{P}^T + e = \hat{X} + e$, with $\hat{X}$ denoting the expected data operating only the reserved principal components and e the model residual given by $X(I_{ki} - \hat{P}\hat{P}^T)$.

Monitoring Metrics with KDE Control Limits

Commonly, the KPCA-based fault recognition utilizes two statistics, the Hotelling T^2 statistics, and the SPE or the Q statistics. The Q metric is mainly preferred for fault identification over the T^2 graph since it is highly resilient to minor flaws. The T^2 statistic is described by the Mahalanobis interval, while the Euclidean distance characterizes the Q statistic.

The Hotelling T^2 of the *j*th samples in the feature space used for KPCA fault exposure is calculated as:

$$T_j^2 = X^T \mathbb{C}^{-1} X \quad (9)$$

where $X = \left[z_{1,j}, \ldots, z_{q,j}\right]$ denotes the PC scores of the jth samples, q is the total of PCs retained and $\mathbb{C}^{-1}$ signifies the inverse of the matrix of eigenvalues consequent to the retained PCs.

The T^2 threshold can also be anticipated from its probability density function (PDF). Kernel density estimation is a strategy for incorporating a dataset with an appropriate streamlined PDF from several random measurements. It is popularly utilized for approximating PDFs, particularly for univariate random data [39]. The KDE is relevant to GLR, T^2, and Q statistics, since they are all univariate, though its framework exemplified by these statistics is multivariate.

Control bounds for evaluating statistics can be computed from their corresponding PDF projections.

$$\int_{-\infty}^{T_\alpha^2} g\left(T^2\right) dT^2 = \alpha \quad (10)$$

Once all scores are of Gaussian distribution, the control bound is related to a significance level, α, and T_α^2 can be originated from F-distribution as:

$$T_\alpha^2 \sim \frac{q(n-1)}{n-q} F_{q,n-q,\alpha} \quad (11)$$

where $F(q, n-q, a)$ is the value of the F-distribution relating to a significance level α, with degrees of freedom q and $n-q$, for both the numerator and denominator.

In addition, a basic calculation of the Q-statistic has been suggested [10]. For the jth samples:

$$Q_j = \sum_{i=1}^{n} z_{i,j}^2 - \sum_{i=1}^{q} z_{i,j}^2 \quad (12)$$

For testing data, an error is confirmed when the limit rate is disrupted as follows:

$$Q_\alpha > C\sqrt{2\varphi_2}\left(1-\frac{2\varphi_1\varphi_3}{3\varphi_2^2}\right)+1+\frac{\varphi_2}{\varphi_1^2}\left(1-\frac{2\varphi_1\varphi_3}{3\varphi_2^2}\right)\left(\frac{2\varphi_1\varphi_3}{3\varphi_2^2}\right) \quad (13)$$

where, $\varphi_i = \sum_{j=l+1}^{i}\lambda_j^i$, $i = 1,2,3 \ \ldots$ and C is the value achieved from the normal distribution of 95% significance.

The KDE control limit is as follows:

$$\int_{-\infty}^{Q_\alpha} g(Q)dQ = \alpha \quad (14)$$

3. SSGLR-Based Monitoring

Hypothesis assessment procedures such as the Generalized Likelihood Ratio (GLR) have acknowledged significant consideration in earlier research [9,12]. Inference methodological processes utilize precise mathematical assumptions to decide whether the data are compatible with or divergent from a prescribed mechanism. The null hypothesis matches a negative distortion, termed an alternate concept. For efficiency evaluation methods, the shortcomings of contingent and self-reliant variable assessments are explicitly defined using examples from standard and irrational operating techniques [1]. The Generalized Probability Ratio model can be utilized for this reason and is discussed in the following section.

The Generalized Likelihood Ratio (GLR) procedure with sequential sampling identifies replacement theories based on parameters that support infinite values and is commonly alluded to as a composite theory. The sequential sampling considered here refers to the situation in which observations are taken one by one. A reasonable quality estimation method that uses the Maximum Likelihood Estimates (MLEs) concept has been used to estimate the appropriate criteria. The SSGLR chart follows the idea of maximum probability projections to optimize the identification frequency with a set untrue warning level. The SSGLR mechanism is carried out in the subsequent section:

1. The zero and alternative assumptions are established, and their corresponding probability features are obtained.
2. All uncertain dimensions in the alternative hypothesis are calculated from the test results through the MLE.
3. The log probability proportion of alternative to null hypotheses is then estimated, and its maximal probability is determined that significantly increases the measurement distance.

Consider at sampling point k we have the data $X_1, \ldots X_k$, where $i = 1,2,\ldots k-1$, $X_i = X_{i1},\ldots X_{ini}$ and there are l observations in sample k. The null assumption once there is no alteration in the mean can be interpreted as:

$$L(\infty,\mu_0|X_1,X_2,\ldots,X_k) = \left(2\pi\delta_0^2\right)^{-\frac{N_{k,l}}{2}} exp\left[-\frac{1}{2\delta_0^2}\sum_{i=1}^{k-1}\sum_{j=1}^{n_i}\left(X_{ij}-\mu_0\right)^2+\sum_{j=1}^{l}\left(X_{kj}-\mu_0\right)^2\right]$$

Assume that a distinct source produces an abrupt change in the procedure amongst the observation τ and $\tau+1$ then parameter μ moves to μ_1 ($\mu_1 \neq \mu_0$) from μ_0, i.e., samples $X_{\tau+1}$, $X_{\tau+2}$, ... are strained from a procedure that is out-of-control with the parameter μ_1. Then, the likelihood function can be presented as follows:

$$L(\tau,\mu_1|X_1,X_2,\ldots,X_k) = \left(2\pi\delta_0^2\right)^{\frac{N_{k,l}}{2}} exp\left[-\frac{1}{2\delta_0^2}\sum_{i=1}^{\tau}\sum_{j=1}^{n_i}\left(X_{ij}-\mu_0\right)^2+\sum_{i=\tau+1}^{k-1}\sum_{j=1}^{n_i}\left(X_{ij}-\mu_1\right)^2+\sum_{j=1}^{l}\left(X_{kj}-\mu_1\right)^2\right]$$

We can attain the maximum likelihood estimation of μ_1, i.e., $\hat{\mu}_1$, through the maximization of $L(\tau, \mu_1 | X_1, X_2, \ldots, X_k)$, which is:

$$\hat{\mu}_{1,\tau,k} = \frac{1}{N_{1,k,l,\tau}} \sum_{i=\tau+1}^{k-1} \sum_{j=1}^{n_i} X_{ij} + \sum_{j=1}^{l} X_{kj} \tag{15}$$

Subsequently, a log likelihood ratio statistic for defining whether there has been a change in the procedure mean in the previous k trials is:

$$R_{k,l} = \ln \max_{0 \le \tau \le k} \frac{L(\tau, \hat{\mu}_1 | X_1, X_2, \ldots, X_k)}{L(\mu_0 | X_1, X_2, \ldots, X_k)}$$

$$R_{k,l} = \max_{0 \le \tau \le k} \frac{N_{1,k,l,\tau}}{2\delta_0^2} (\hat{\mu}_{1,k,l,\tau} - \mu_0)^2$$

In calculating $R_{k,l}$, we must track all previous data points from samples 1 to k in addition to finding the maximum, which entails large computation when k is big. A window of size m pertaining to the maximization in $R_{k,l}$ is occupied only over the past m samples.

The SSGLR statistic can be then expressed as:

$$R_{k,l,m} = \max_{max\ (0,k-m)} \frac{N_{1,k,l,\tau}}{2\delta_0^2} (\hat{\mu}_{1,k,l,\tau} - \mu_0)^2 \tag{16}$$

The SSGLR control chart decision rule calls for specifying two limits, g and h, which satisfy the condition $0 < g < h$, where g is the limit that tells when it is time to stop sampling at the present point of sampling while h is the control limit. This is how the decision rule is defined. Taking k to be the current sampling point and l as the present sum of observations at the specified sampling point:

A. Evaluate R_{mkl}.
B. If $R_{mkl} \le g$, it means that at the sampling point k, you will stop sampling and then wait until you reach sampling point k+1 to re-sample. Therefore, the sample size at the k sampling point here is now $n_k = l$.
C. If $g < R_{mkl} < h$, we have two options that we need to follow, which include:
   (i) Taking the subsequent observation at the sampling point *k;*
   (ii) Moving to step A, which is given above with the present sum of observations at the k sampling point provided as $l = l + 1$.
D. In case $R_{mkl} > h$, it signals that the process vector mean μ has experienced a change.

You can choose the control chart parameters h and g to meet the in-control performance requirements that have been specified.

If $\acute{R}_{k,m,l}$ falls outside the interval $\left[\acute{h}_{GLR}\delta_0, \acute{g}_{GLR}\delta_0\right]$, then the chart will trigger a signal. The KDE control limit can be obtained by using the equation below:

$$\int_{-\infty}^{\acute{h}_{GLR}\delta_0} g(\acute{R}_{k,m,l}) d\acute{R}_{k,m,l} = \alpha \text{ and } \int_{-\infty}^{\acute{g}_{GLR}\delta_0} g(\acute{R}_{k,m,l}) d\acute{R}_{k,m,l} = \alpha \tag{17}$$

4. Fault Monitoring Using KPCA-KDE-SSGLR

This research does establish a detection technique to identify a diverse variety of process shifts for nonlinear multivariate frameworks. Significantly, the suggested approach combined KPCA-KDE and GLR statistics using sequential sampling. Figure 1 shows the flow chart of the KPCA-KDE-SSGLR procedure. The KPCA is considered to minimize the dimensionality in the procedure, and the SSGLR is being used as a tracking statistic. The current technique consists of two stages, stage I for offline training and stage II for online fault detection. Step 1 uses standard data to create a measurement structure and approximate the related parameters. For Step 2, new data obtained through the virtual

system are being used to determine the system's state; details of the two phases are given below.

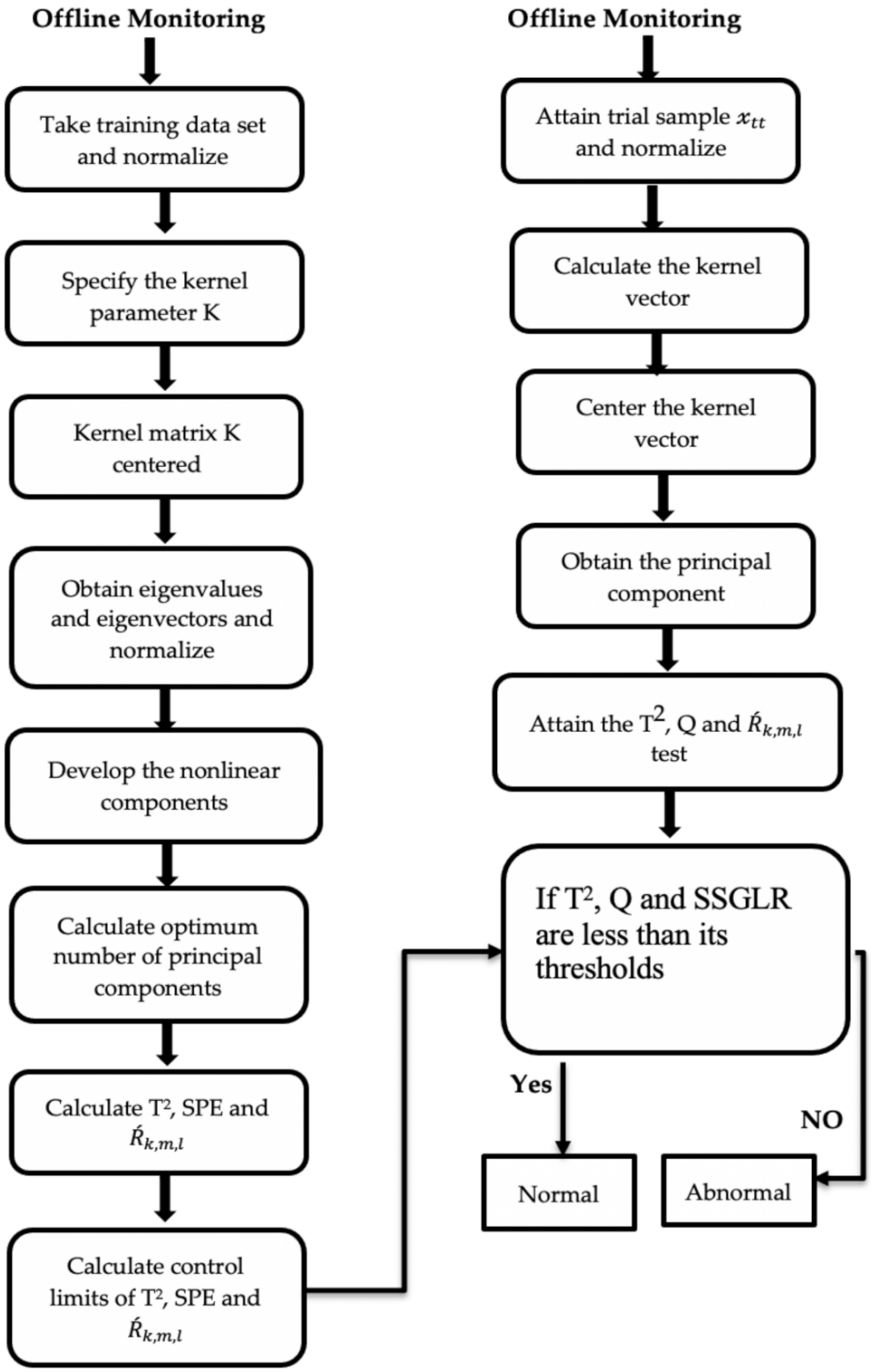

Figure 1. Flowchart of KPCA-KDE-SSGLR monitoring.

4.1. Offline Model Development

1. Collect the results during normal operating conditions (NOC) and level the dataset utilizing the mean and standard deviation of the sample collection sections describing different variables.

2. Pick the type of kernel structure to be used and specify the kernel parameter.
3. Develop and cluster the kernel module of the NOC dataset utilizing Equation (5).
4. Attain eigenvalues and their consistent eigenvectors then reorganize in a descendent direction.
5. Orthonormalize the eigenvectors employing Equation (6).
6. Achieve nonlinear modules by applying Equation (7).
7. Calculate the optimum number of principal components to be utilized by CPV.
8. Calculate monitoring indices $\acute{R}_{k,m,l}$, T^2 and Q grounded on the kernelized NOC data through Equations (9), (12) and (16).
9. Accomplish control limits of $\acute{R}_{k,m}$, T^2 and Q by Equations (10), (14) and (17).

4.2. Online Monitoring

1. Attain trial sample $\S_{tt}$ and stabilize utilizing the mean and standard deviation standards exercised in step 1 of the offline stage.
2. Calculate the kernel vector of the trial sample utilizing the below equation:

$$[k_{tt}] = k(\S_i\ , \S_{tt}) \tag{18}$$

3. Center the kernel vector as per the equation given below:

$$\mathbf{K}_{ctt} = \mathbf{K}_{tt} - u_1\mathbf{K} - \mathbf{K}_{tt}U + u_1\mathbf{K}U \tag{19}$$

4. Obtain the principal component of the test sample from by utilizing the equation:

$$z_{tt,k} = \sum_{i=1}^{n} \alpha_{k,i}[\mathbf{K}_{ctt}]_i \tag{20}$$

5. Attain the T^2 and Q of the test sample with their individual control limits acquired in the model improvement phase.
6. Analyze the charting statistics $\acute{R}_{k,m,l}$.
7. If $\acute{R}_{k,m,l} > \mathrm{UCL_R}$ then it specifies an unstable condition occurring in the procedure and the expert must instantaneously find out the root causes and resolve it.
8. The process is in-control if both T^2 and Q are smaller than their scrutinizing values. If either T^2 or Q surpasses its threshold, the procedure is out-of-control and consequently, fault identification is conceded to distinguish the basis of the fault.

To appropriately assess the outcomes [12,40] the fault detection rate (FDR) and false alarm rate (FAR) are described as follows:

$$FDR = \frac{AN}{TAN} \text{ and } FAR = \frac{NN}{TNN}$$

Whenever the procedure is normal, NN is the number of defective instances which are assessed. The cumulative number of normal trials is TNN, the amount of faulty data is AN when the procedure is faulty, and the total number of anomalous samples is TAN.

5. Synthetic Data Example

Through this illustration, the superior SSGLR malfunction prevention methodology's efficiency-focused KPCA-KDE is evaluated through recognizing faults in the process. The KPCA-KDE-based SSGLR model is assessed in magnitude unity mean shift condition, using two illustrative examples: the modeled simulated data collection [40,41] and the Tennessee Eastman Process benchmark (TEP). Three fault detection metrics are used to measure efficiency, fault detection rate (FDR), false alarm rate (FAR), and average run length (ARL_1).

Data Generation

The outputs of three variable vectors as functions of time x_1, x_2, x_3 are obtained utilizing the simulated model as given below:

$$x_1 = -1 \times ones(400,\ 1); 2 \times ones(600,\ 1)$$

$$x_2 = \sin(0.1 : 0.1 : 100)^T + \cos(0.1 : 0.1 : 100)^T$$

$$x_3 = x_1^2 + x_2^2 + 0.3 \times \sin(2\varphi x_1)$$

The distortion in these modeled scenarios is considered to be zero. They are then polluted with zero mean Gaussian errors, i.e., measurement noise $v_{k-1} \sim \left(0,\ \delta_v^2\right)$, resulting in:

$$X_1 = x_1 + \epsilon_v \times randn(size(x_1))$$

$$X_2 = x_2 + \epsilon_v \times randn(size(x_2))$$

$$X_3 = x_3 + \epsilon_v \times randn(size(x_3))$$

Training data of 1000 and testing data of 600 samples each are produced utilizing the model above. The created data were organized as a matrix $\mathbb{X} = [\mathbb{X}_1, \mathbb{X}_2, \mathbb{X}_3,]$ having 1000 illustrations and three variables. The responses of the three state variables $\mathbb{X}_1, \mathbb{X}_2,$ and $\mathbb{X}_3,$ are displayed in Figure 2.

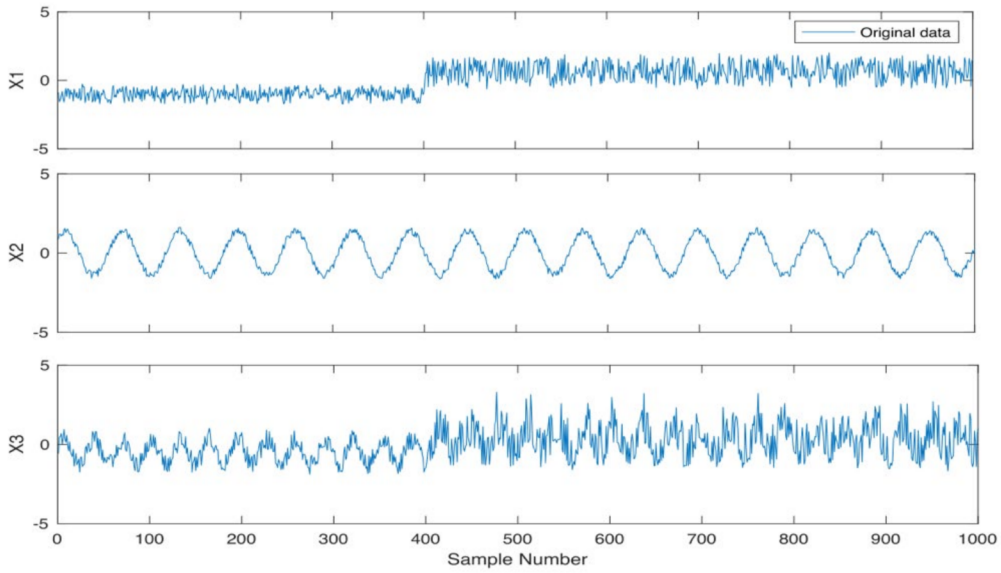

Figure 2. The time evaluation of generated data.

As asserted in the methodology, fault-free series training data were employed to create a KPCA standard framework for malfunction classification. The fault-free design dataset was structured as an $\mathbb{X}_{tt}$ matrix with 600 measurements and three model variables. These measurements were first standardized (zero mean and unit variance) and then employed to create the KPCA structure. Responses to the fault-free training results are displayed in Figure 3.

In KPCA, several primary variables in the dataset are usually recorded in the principal PCs contributing to the maximal eigenvalues, as shown in Figure 4. This analysis uses the CPV procedure to assess the optimal number of PCs maintained. The CPV approach is employed to determine the optimal number of retained PCs with a threshold value of 95%, resulting in three PCs' retention.

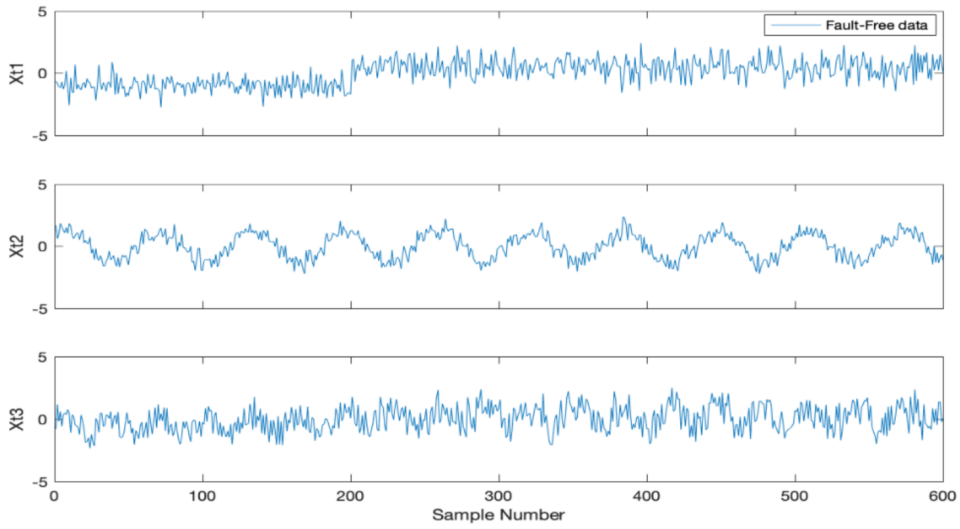

Figure 3. The time evaluation of fault-free data.

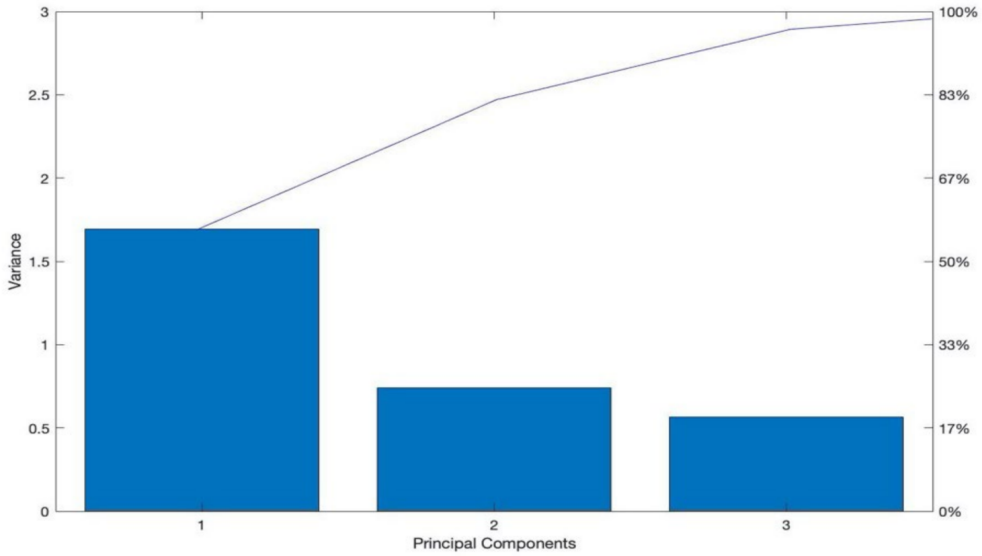

Figure 4. Variance gained by each principal component.

Case 1. No-fault

The detection approaches, including SSGLR, T^2 and Q statistics, are first conducted utilizing the training fault-free data $\mathbb{X}_{tt}$ (Figure 3). It can be observed from Figure 5a–c, that the SSGLR, T^2 and Q statistics are continuously underneath the limit standards. The dotted and dashed lines denote the control limits at 99% confidence level grounded on Gaussian distribution and KDE, correspondingly. From Figure 5, it can be observed that the data fit the KPCA model satisfactorily (because it can catch maximum deviations in the data), and approves that the procedure works under ordinary situations, where no faults are existent.

Case 2: Mean shift of magnitude unity

This condition explores all fault diagnosis charts' efficiency where a continuous step breakdown in the mean of amplitude unity is present from measurements 300 to 600. This degree of phase flaw was selected to demonstrate appropriate identification using the KPCA-KDE-based Q chart and allow the output of the KPCA-KDE-SSGLR figures to be contrasted and investigated.

The outcomes of the error identification for the KPCA-KDE-based T^2 and Q charts are presented in Figure 6b,c. According to the severity of the defect, the KPCA-KDE-based T^2

map cannot locate the whole fault efficiently (see Figure 6c), whereas the KPCA-KDE-based Q chart (see Figure 6b) can accomplish substantially stronger identification.

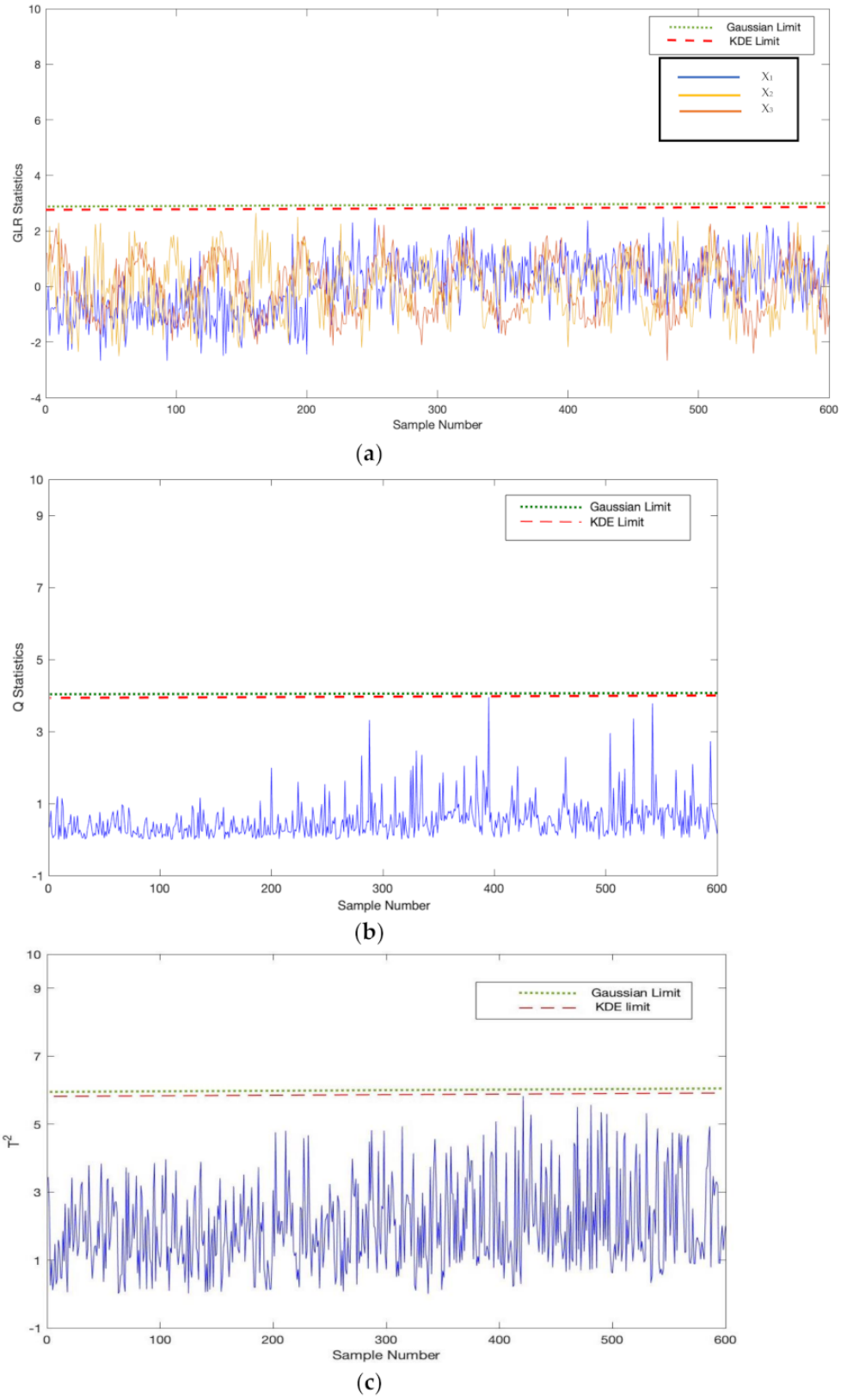

Figure 5. (**a**) KPCA-KDE-based SSGLR charts for the fault-free data; (**b**) KPCA-KDE-based Q chart for the fault-free data; (**c**) KPCA-KDE-based T^2 chart for the fault-free data.

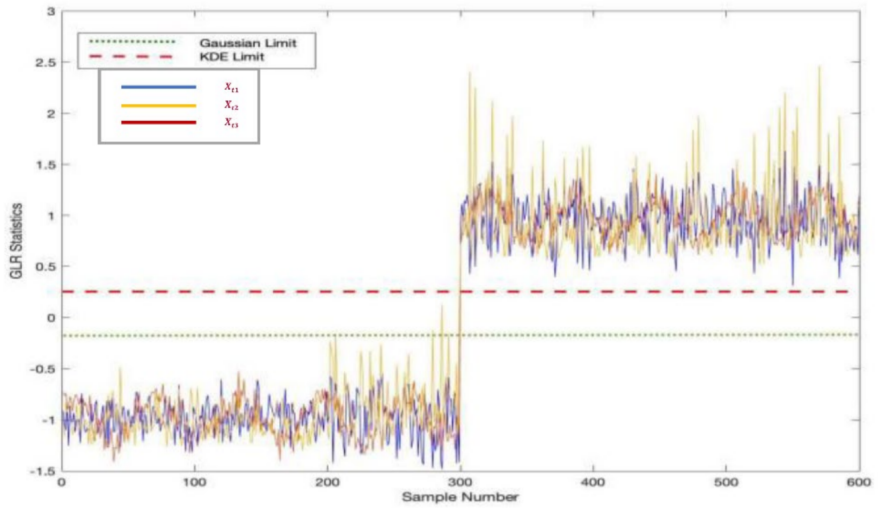

(**a**)

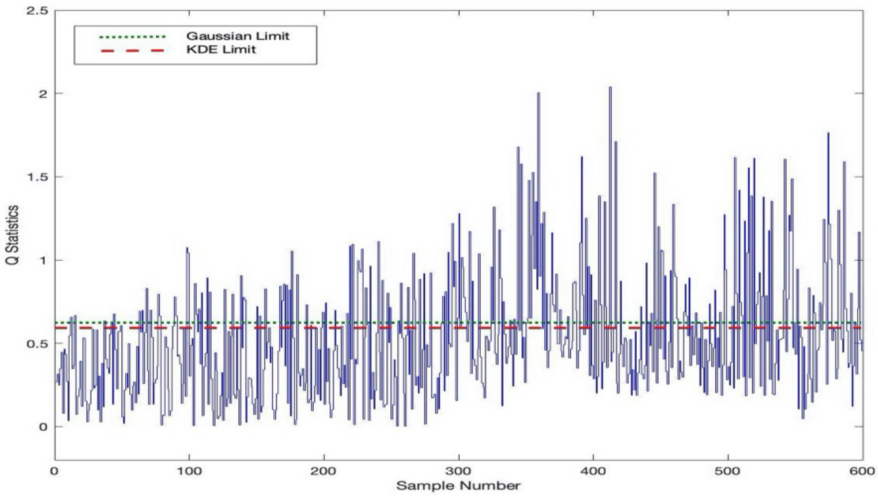

(**b**)

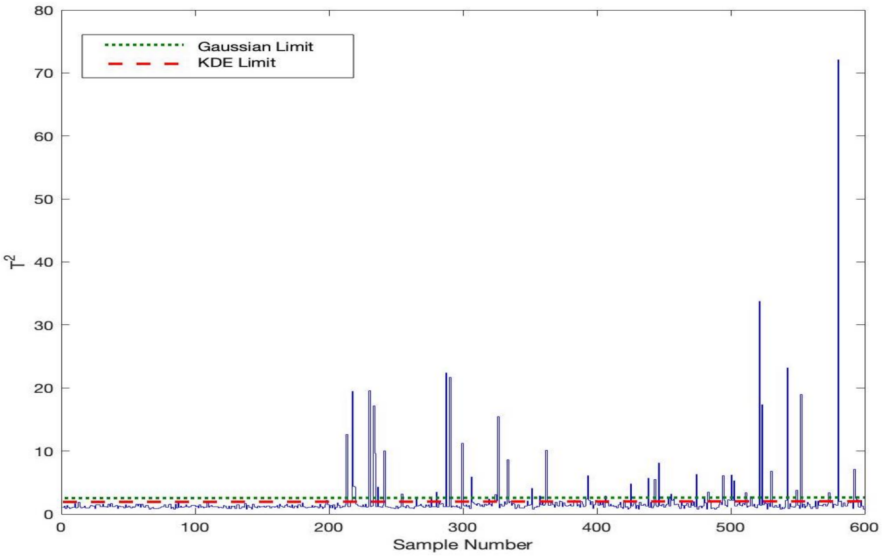

(**c**)

Figure 6. (**a**) KPCA-KDE-based SSGLR charts; (**b**) monitoring fault using KPCA-KDE-based Q chart; (**c**) monitoring fault using KPCA-KDE-based T^2 chart.

The KPCA-KDE-based SSGLR chart proposed to identify changes in the mean presented in Figure 6a displays that the SSGLR chart considered mainly to spot changes in the mean is capable of detecting the whole fault, with minimum missed detections.

It can be perceived that the KDE-based control bounds are underneath the Gaussian distribution-based control bounds for T^2 and Q charts, while it is above the Gaussian limit as in the case of SSGLR statistics. In other words, the tracking indicators surpass the KDE-based threshold values to a larger extent than the Gaussian distribution-based thresholds. This suggests that KDE-based control levels for the KPCA methodology result in better tracking efficiency relative to Gaussian distribution-based constraints.

Assessing the overview of the findings of the failure identification, Table 1 shows that the KPCA-KDE-SSGLR chart constructed to evaluate changes in the mean offered the most considerable false detection rate (FDR) and gives a minimal ARL_1 value relative to the T^2 statistic and the Q statistic.

Table 1. Summary of fault detection results.

	FDR (%)	FAR (%)	ARL_1
KPCA-KDE-based T^2	14.47	2.71	1.025
KPCA-KDE-based Q	40.58	5.87	5.50
KPCA-KDE-SSGLR	99.50	0.07	3.55
KPCA-based T^2	11.58	2.50	1.025
KPCA-based Q	40.58	9.46	5.50
KPCA-based GLR	96.40	13.80	3.55

From the outcomes displayed in Table 1, it can be seen that the KPCA-KDE-SSGLR graph explicitly developed to discover shifts in the mean exceeds almost all statistics in context of the false detection level, whereas it offers nearly equivalent ARL_1 values to other methods. The KPCA-KDE-SSGLR shows excellent performance, as can be seen from Table 1 its false detection rate is as high as 99.50%, whereas KPCA-based T^2 has only an 11.58% false detection rate. This shows that KPCA can perform much better by integrating it with the SSGLR statistic. The SSGLR statistics already proved to have much better performance in terms of ARL [4,8]. Moreover, the findings demonstrate that KDE control bounds editions obtain a substantially higher error detection accuracy relative to the consequent Gaussian distribution-based models. In addition, Table 1 shows that the missed prevalence estimates of KDE-based models are mainly equivalent to or lesser than non-KDE-based methodologies. This assumes that KDE-based initiatives to UCLs identified flaws relatively earlier than their Gaussian distribution-based counterparts. Affiliating the KDE-based threshold values with the KPCA failure detection method gives excellent tracking, especially compared to using the Gaussian accusation critical bounds.

6. Tennessee Eastman Process (TEP)

In an attempt to scrutinize the usefulness of employing the KPCA-KDE-SSGLR graph for tracking mechanism mean variations, its consistency needs to be measured utilizing actual data. Many writers use the Tennessee Eastman Process (TEP) to test the efficiency of their procedures [12,25,35]. The Tennessee Eastman Process is a practical model of the natural chemical compound consisting of a generator, condenser, stripper, compressor, and separator, and is generally recognized as a paradigm for fault identification [25].

The Tennessee Eastman Method includes a database of predetermined flaws that researchers can use to test the efficiency of their designed flaw detection techniques. Further details on the Tennessee Eastman Process, the overview of the procedure, and the accessible defect database can be found in the literary works [4,12,25,35]. This research investigates the fault situation Fault 12 of the TE method. Fault 12 (IDV12) is a random variation in the condenser cooling water inlet temperature.

Fault Situation: IDV 12, Random Variation in the Cooling Water Inlet Temperature

This particular fault scenario implemented the 3 h of purposeful alteration in the inlet cooling water temperature. The KPCA-KDE-based T^2 and Q charts and the KPCA-KDE-SSGLR statistics are shown in Figure 7a–c, and the failure conclusions designation is tabulated in Table 2.

Table 2. Summary of fault detection results (TEP: IDV 12).

	FDR (%)	FAR (%)	ARL_1
KPCA-KDE-based T^2	10.18	6.10	45.00
KPCA-KDE-based Q	23.36	0.27	148.00
KPCA-KDE-SSGLR	81.35	7.13	70.00
KPCA-based T^2	09.87	9.52	45.00
KPCA-based Q	12.69	0.25	148.00
KPCA-based GLR	78.67	10.36	70.00

From Figure 7b,c, it can be confirmed that perhaps the T^2 and Q-based KPCA-KDE statistics are not worthy of tracking the entire fault. Fascinatingly, the KPCA-KDE-SSGLR chart developed primarily to examine mean alterations (see Figure 7a) can identify a considerable number of defects with the lowest missing identification accuracy.

From the outcomes displayed in Table 2, it can be observed that the KPCA-based Q statistic has a few low false alarm rate, 0.25%, but its false detection rates are too low compared to all other statistics. The false detection rate (FDR) of KPCA-KDE-SSGLR is 81.35%, which is much higher compared to all other charts. Therefore, it can be perceived from Table 2 that the KPCA-KDE-SSGLR process is much superior to its counterparts, such as KPCA-based T^2 and Q statistics.

The KPCA-KDE-based T^2 statistic has a much smaller ARL_1 value but cannot adequately locate a number of the visible faults, and so the smaller ARL_1 value can be related to the noise signal.

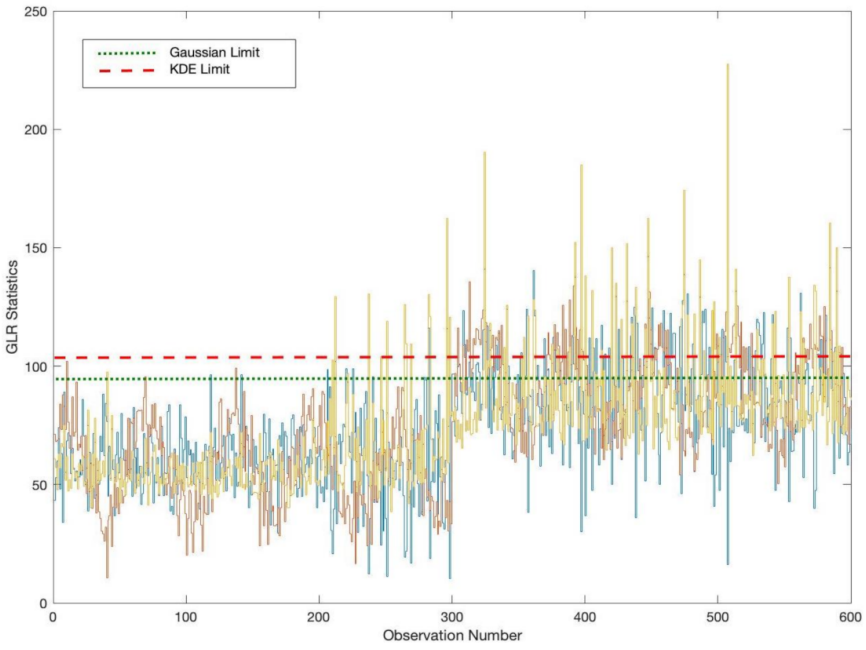

(**a**)

Figure 7. *Cont.*

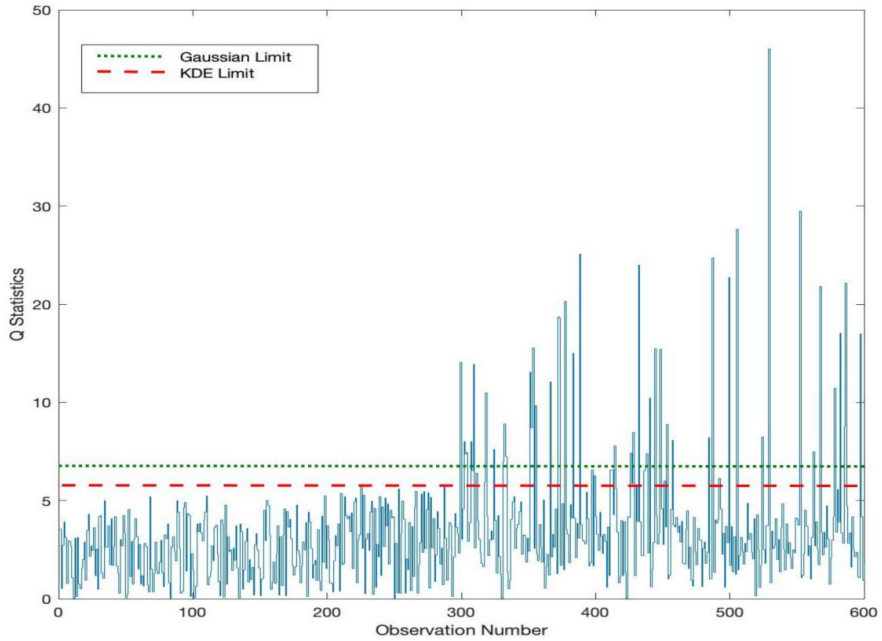

(**b**)

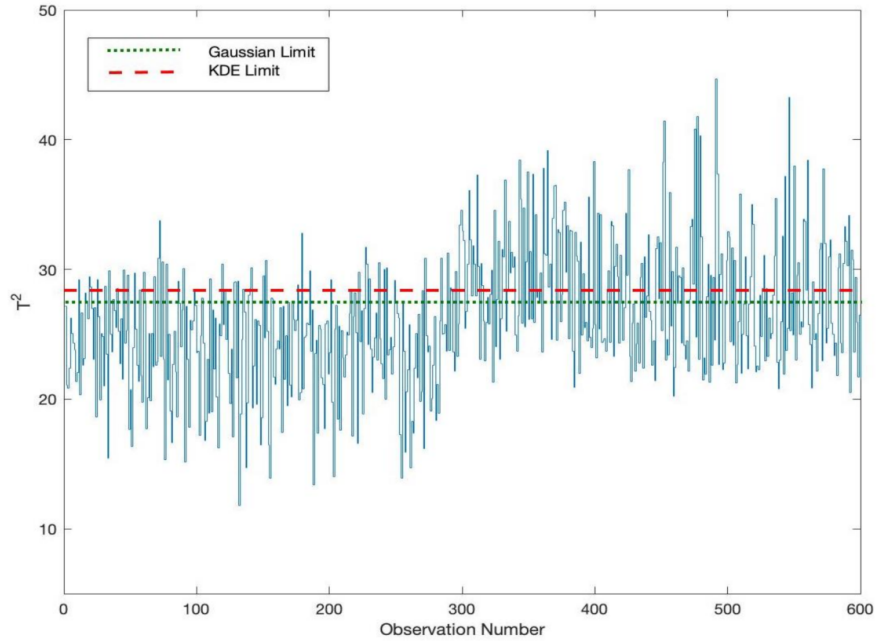

(**c**)

Figure 7. (**a**) Monitoring fault IDV 12 using KPCA-KDE-SSGLR chart; (**b**) monitoring fault IDV 12 using KPCA-KDE based Q chart; (**c**) monitoring fault IDV 12 using KPCA-KDE based T^2 chart.

7. Comparison of KPCA-KDE-SSGLR with KLPP for Hot Strip Mill

Suppose the HSM fault identification is to be disseminated. In that case, the data acquisition scheme for the inspecting indication must be established initially, and various accumulating methods and procedures for different signal types should be performed.

A hot strip mill is a highly complicated efficient production practice. Optimizing product eminence can provide the manufacturer with long-term economic and societal benefits.

There are numerous different monitoring and supervision signals for a particular HSM platform, making it hard for us to choose all of them.

In the finishing mill division, there are typically seven stand mill units. Each mill stand comprises an active roll, a standing arch, a reserve roll, the hydraulic screw-down, work

roll bending, and balance and backup roll balance devices. A big AC motor generally drives every mill. The precision controls of the hydraulic servo system primarily complete the roll gap among upper and lower work rolls, so that a specified thickness of strip can be the exit thickness after such mill. A texture gauge, thermometer, breadth gauge, flatness gauge, and other devices are commonly found near the exit of the finishing machine. Automatic gauge control (AGC), finishing temperature control (FTC), and automatic slab control (ASC) are frequently included in the rolling mill control system to ensure that the exit thickness, temperature, and flatness comply with the requirements. Low-inertia hydraulic loops are typically installed amongst stands to manage strip micro-tension. This maintains the mass flow of each strip stably, allowing for smooth high-speed rolling. After completing seven stands of high-speed cruising, the strip length grows dramatically. After laminar cooling at the proper temperature to the appropriate temperature, strip winds form the final product.

AGC has to be the most effective component for dynamic thickness control in traditional rolling mills. The AGC system is meant to minimize disorders throughout the rolling phase, such as strip roughness and temperature fluctuations, because it is accountable for preserving the dynamic response of the projected thickness standard. The incredibly complicated methods were created to accomplish the goal of active thickness management, while the idea and attitudes for tuning were established separately.

We choose process variables such as roll force, roll gap, roll bending force, and delivery thickness based on the gauge's primary parameters. To test the algorithm's performance, we only use the 12 AGC-related indications or measured variables, as well as one quality variable, as shown in Table 3.

Table 3. AGC-related signals.

No.	Signal Name	Number of Signals
1	Four FM stands roll gap	4
2	Four FM stands roll force	4
3	Four FM stands roll bending force	4
4	Finishing mills exit strip thickness	1

The training dataset consists of 150 coils rolled with the proper roll gap values. There are 32 normal sets and 115 fault sets in the testing dataset. The first 1500 samples are collected as modeling data to investigate the causes.

Fault 1 is that due to the stoppage of the hydraulic instrument in the third stand bending roll route, the scheming roll bending force does not comply with the current one, as shown in Table 4. The flaw is a phase that will change the contour of the outlet strip, but it will have little impact on the thickness, and therefore it is non-pertinent in terms of quality.

Table 4. Information of faults.

Fault No.	Description	Type
1	Blending force sensor fault	quality non-pertinent
2	Cooling valve fault	quality pertinent

Fault 2 is that the cooling valve amongst the first and second stands could not be stopped during the setup mode. At the second stand entry, the strip temperature is low, resulting in positive divergence. It impacts the thickness of the product, so it is essential in terms of quality.

We used false alarm rate (FAR) and fault detection rate (FDR) to showcase practical outcomes to evaluate different techniques. Table 5 summarizes the findings.

Table 5. False detection/alarm rate and ARL_1 of KPCA-KDE-SSGLR and KLPP.

	FDR (%)	FAR (%)	ARL_1.
KPCA-KDE-based T^2	17.18	8.20	76.30
KPCA-KDE-based Q	20.36	6.32	130.00
KPCA-KDE-SSGLR	98.64	1.21	50.64
KLPP-based T^2	80.35	17.74	105.00
KLPP-based Q	85.29	22.05	160.00

Table 5 shows that both T^2 and SPE process metrics in KLPP are incompetent to differentiate between normal and fault batches. Both T^2 and SPE charts in KPCA-KDE produce a notable FAR, and the KPCA-KDE can efficiently differentiate between normal and fault sets, as shown in Figure 8a,b and Figure 9a,b. The best monitoring result is achieved with a recognition rate of 85.29% with the KLPP-based Q chart, whereas Table 5 demonstrates that the KPCA-KDE-based SSGLR chart has the best overall efficiency. It indicates that KPCA-KDE-based SSGLR generates very few FAR, and ARL_1 is also less. The best monitoring result has a detection accuracy of 98.64%; however, KLPP has an accuracy of 85.29%.

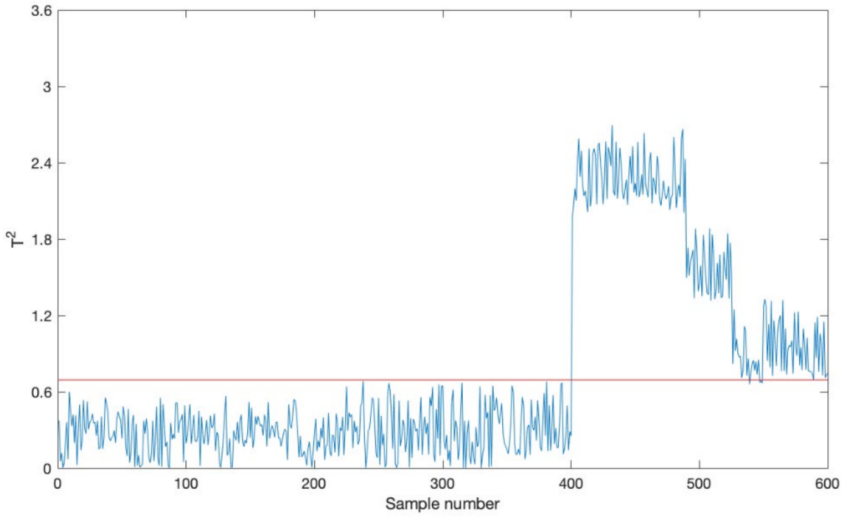

(**a**)

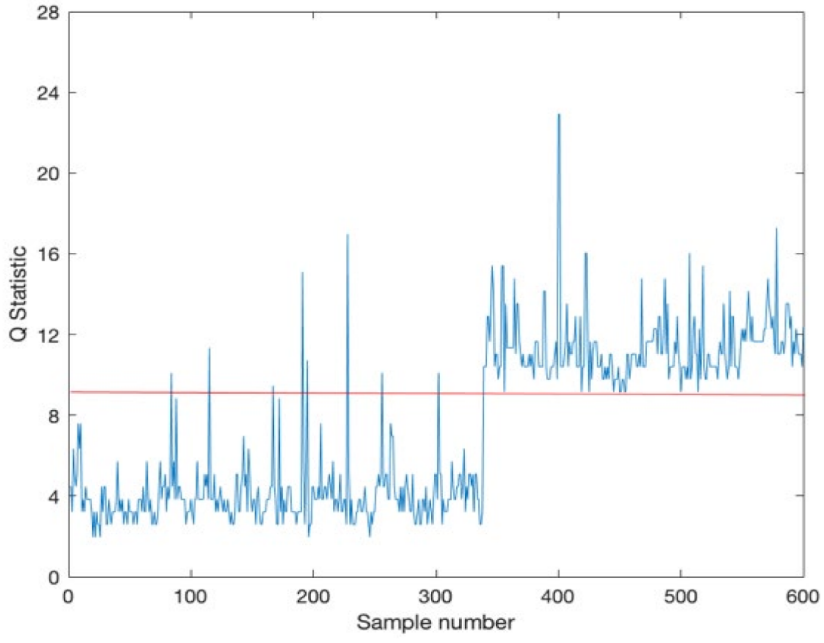

(**b**)

Figure 8. *Cont.*

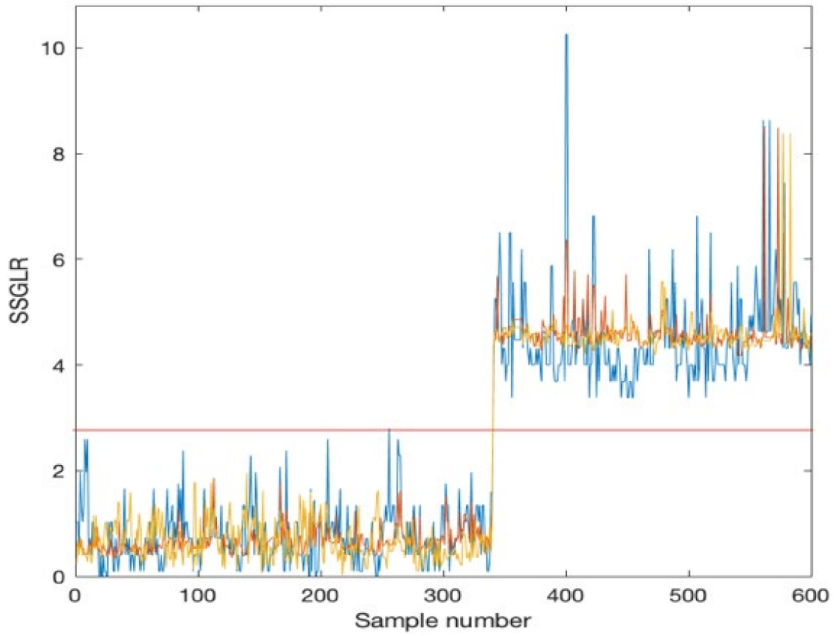

(**c**)

Figure 8. (**a**) KPCA-KDE based T^2 chart fault detection results in quality non-pertinent; (**b**) KPCA-KDE-based Q chart fault detection result in quality non-pertinent; (**c**) KPCA-KDE-based SSGLR chart fault detection result in quality non-pertinent.

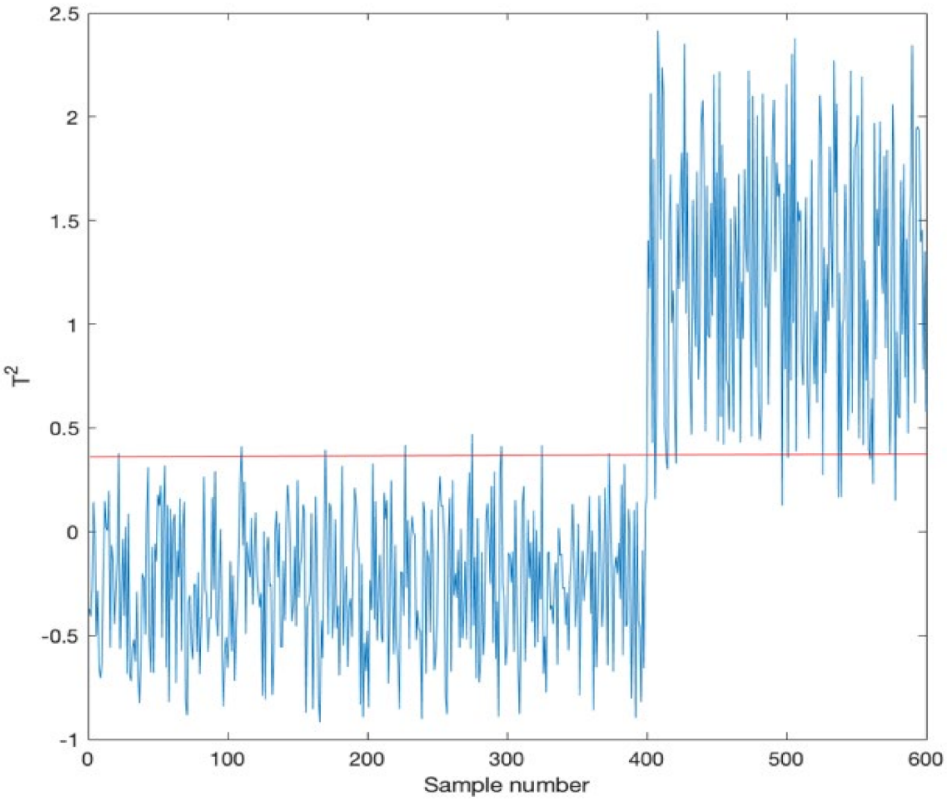

(**a**)

Figure 9. *Cont*.

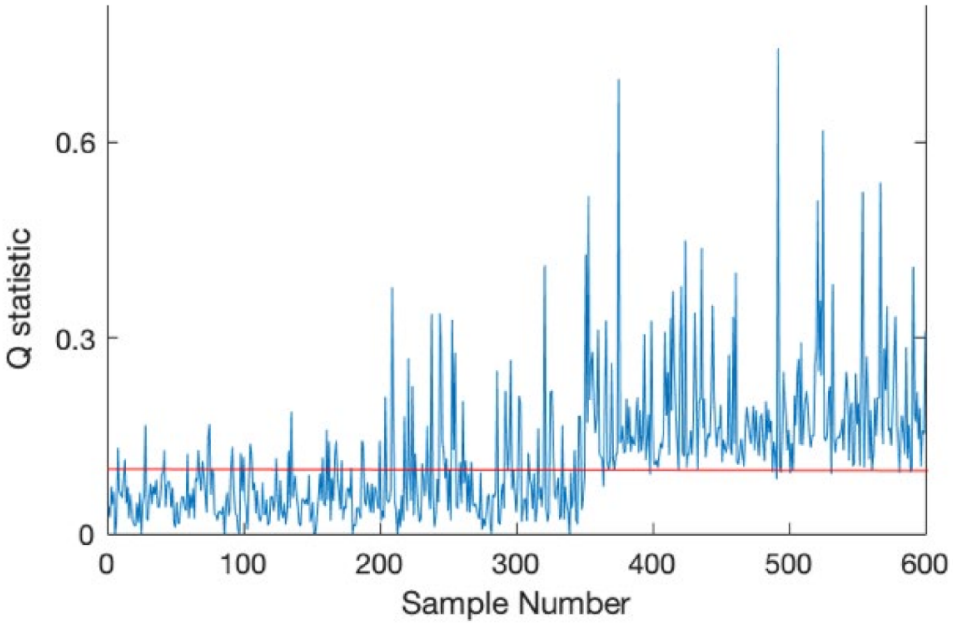

(**b**)

Figure 9. (**a**) KLPP-based T^2 chart fault detection results in quality non-pertinent; (**b**) KLPP-based Q chart fault detection results in quality non-pertinent.

Figures 8–11 illustrate the related simulation graphs. FDR is higher with KPCA-KDE-SSGLR, while FAR is nearly the same.

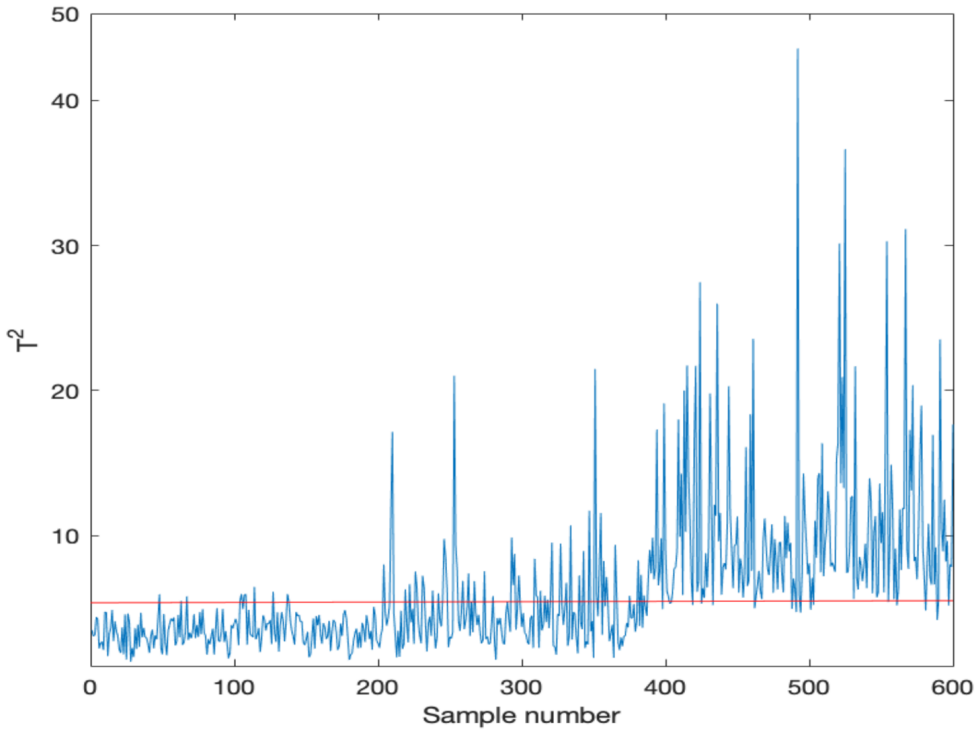

(**a**)

Figure 10. *Cont*.

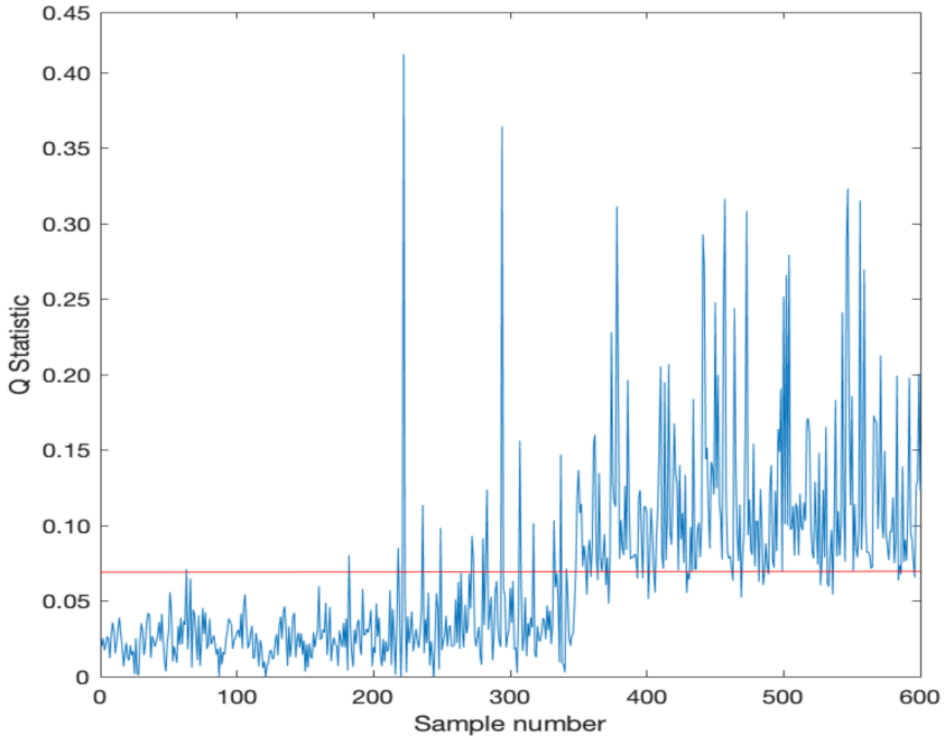

(**b**)

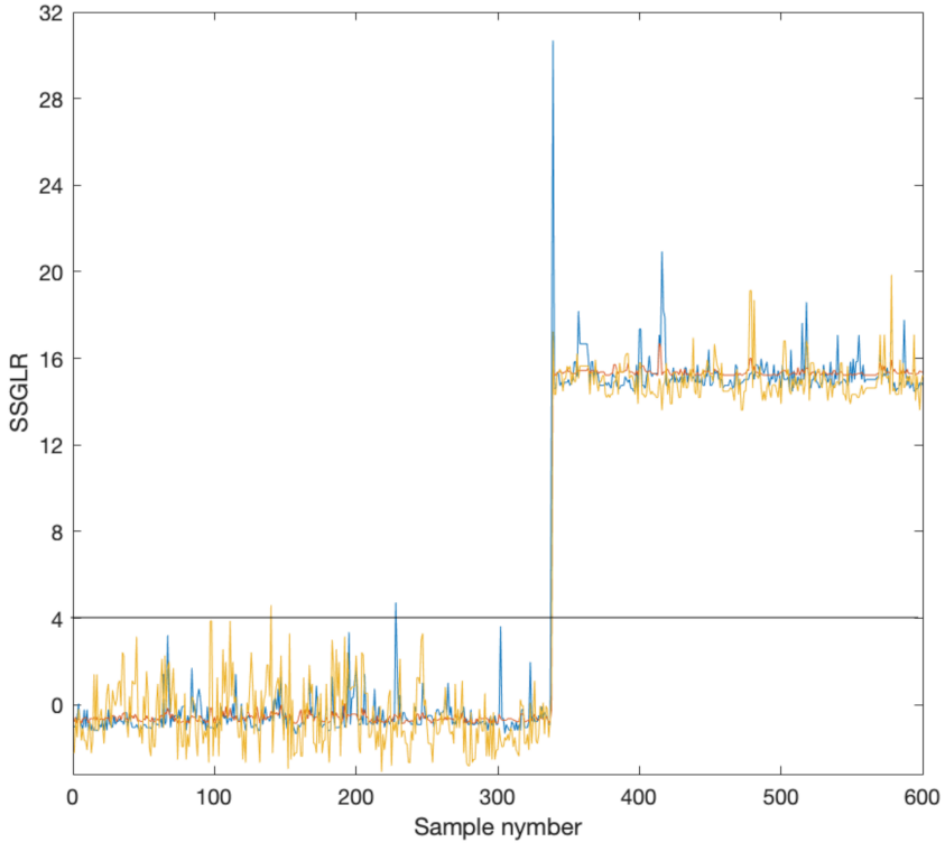

(**c**)

Figure 10. (**a**) KPCA-KDE-based T^2 chart fault detection results in quality pertinent; (**b**) KPCA-KDE-based Q chart fault detection results in quality pertinent; (**c**) KPCA-KDE-based SSGLR chart fault detection results in quality pertinent.

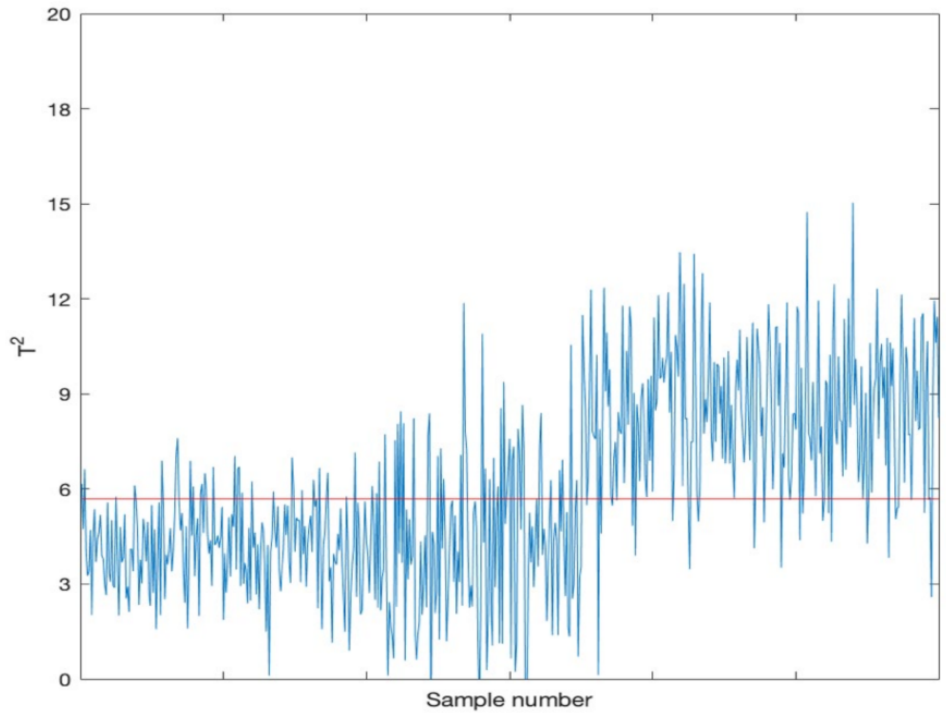

(**a**)

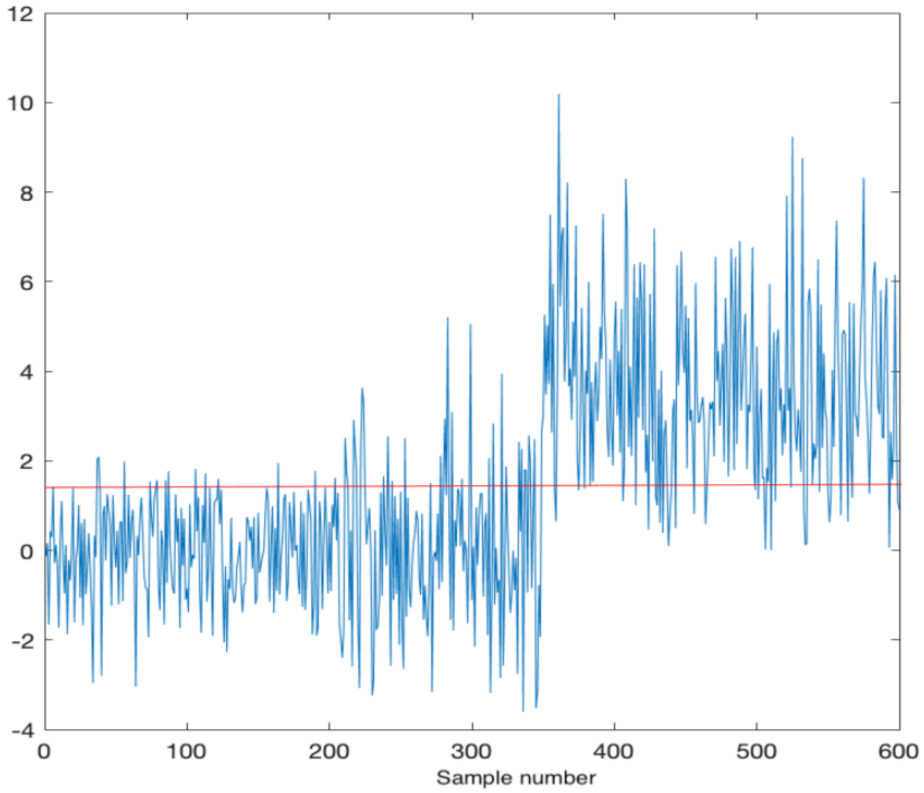

(**b**)

Figure 11. (**a**) KLPP-based T^2 chart fault detection results in quality pertinent; (**b**) KLPP-based Q chart fault detection results in quality pertinent.

As a result, KPCA-KDE-SSGLR should be adequate for finding more significant inherent information buried in observations. For this reason, the model developed here might be contemplated as a valuable means for detecting nonlinear faults in stream processing.

8. Concluding Remarks

This article analyzes highly nonlinear fault monitoring and recognition using the KPCA-KDE methodology. The Kernel Principal Components Analysis (KPCA)-based Generalized Likelihood Ratio (GLR) index is used for variational defect identification using a sequential sampling plan. The malfunction tracking issue was addressed so that the data are first patterned using the KPCA strategy, and afterward, the flaws are analyzed utilizing SSGLR statistics. The KPCA mechanism was thus evaluated as a forecasting algorithm for error tracking tasks. Throughout this study, the limits used to create the control charts were generated explicitly from its PDFs of the tracking metrics rather than applying limits depending on the Gaussian distribution. The fault tracking efficiency of the KPCA-KDE-based SSGLR was evaluated and correlated to that of the standard KPCA methodology centered on Gaussian assumptions by two instances: the synthetic data and the Tennessee Eastman method. Additionally, the hot strip rolling procedure was used to validate the performance of the proposed KPCA-KDE-SSGLR technique over the KLPP method.

The findings illustrate the viability of the KPCA-KDE-based SSGLR methodology over the KLPP and the KPCA through its two T^2 and Q charts for nonlinear fault detection. In particular, the research substantiates the assertion that the use of KDE-based critical bounds and the SSGLR process provides more substantial tracking outcomes in nonlinear procedures than Gaussian-based critical bounds and the KLPP process.

By using KDE control limits and integration of KPCA with the SSGLR statistic for monitoring faults in industries, nonlinear fault detections can be improved dramatically. The importance of manufacturing zero-defect coils in the face of increasing global competition in the steel processing industries cannot be underestimated.

As future study, the bootstrap re-sampling method [42] can be employed to estimate the control limit of the proposed method. Development of the mixed kernel function can also be a good alternative to exchange the conventional kernel used in this study. Still, somehow there are certain unanswered concerns that remain to be addressed in further research, such as how to pick the ideal values of variables, an essential topic in this study for the aim of model validation. Additionally, because it is of considerable practical importance, the study into how to categorize the discovered irregularity as a specific root-cause breakdown offers a major problem for process engineers.

Author Contributions: Conceptualization, methodology, software, resources, writing—original draft preparation, writing—review and editing, F.S.; Investigation and supervision, Z.H.; visualization, W.H.M. All authors have read and agreed to the published version of the manuscript.

Funding: This research received no external funding.

Institutional Review Board Statement: Not applicable.

Informed Consent Statement: Not applicable.

Data Availability Statement: Not applicable.

Conflicts of Interest: The authors declare that they have no conflict of interest to report regarding the present study.

References

1. Shewhart, W.A. *Economic Control of Quality of Manufactured Product*; Macmillan and Co., Ltd.: London, UK, 1931.
2. Page, E.S. Continuous inspection schemes. *Biometrika* **1954**, *41*, 100–115. [CrossRef]
3. Roberts, S.W. Control Chart Tests Based on Geometric Moving Averages. *Technometrics* **1959**, *1*, 239–250. [CrossRef]
4. Montgomery, D.C. *Introduction to Statistical Quality Control*, 6th ed.; John Wiley & Sons, Inc.: Hoboken, NJ, USA, 2009.
5. Yang, K.; Jayant, T. *Multivariate Statistical Methods in Quality Management*; McGraw-Hill Education: New York, NY, USA, 2004.
6. Hotelling, H. The generalization of Student's ratio. *Ann. Math. Stat.* **1931**, *2*, 360–378. [CrossRef]
7. Healy, J.D. A note on multivariate CUSUM procedures. *Technometrics* **1987**, *29*, 409–412. [CrossRef]
8. Lowry, C.A.; Woodall, W.H.; Champ, C.W.; Rigdon, S.E. A multivariate exponentially weighted moving average control chart. *Technometrics* **1992**, *34*, 46–53. [CrossRef]

9. Wang, S.; Reynolds, M.R., Jr. A GLR control chart for monitoring the mean vector of a multivariate normal process. *J. Qual. Technol.* **2013**, *45*, 18–33. [CrossRef]
10. Xu, L. The Design of GLR Control Charts for Process Monitoring. Ph.D. Thesis, Virginia Tech, Blacksburg, VA, USA, 2013.
11. Huang, W.; Wang, S.; Reynolds, M.R., Jr. A generalized likelihood ratio chart for monitoring Bernoulli processes. *Qual. Reliab. Eng. Int.* **2013**, *29*, 665–679. [CrossRef]
12. Shahzad, F.; Huang, Z.; Shafqat, A. The Design of GLR Control Chart for Monitoring the Geometric Observations Using Sequential Sampling Scheme. *Symmetry* **2020**, *12*, 1964. [CrossRef]
13. Reynolds, M.R., Jr.; Lou, J. An evaluation of a GLR control chart for monitoring the process mean. *J. Qual. Technol.* **2010**, *42*, 287–310. [CrossRef]
14. Apley, D.W.; Shi, J. The GLRT for statistical process control of autocorrelated processes. *IIE Trans.* **1999**, *31*, 1123–1134. [CrossRef]
15. Lai, T.L. Sequential analysis: Some classical problems and new challenges. *Stat. Sin.* **2001**, *11*, 303–351.
16. Lee, J.M.; Yoo, C.K.; Lee, I.B. Statistical process monitoring with independent component analysis. *J. Process Contr.* **2004**, *14*, 467–485. [CrossRef]
17. Ge, Z.Q. Review on data-driven modeling and monitoring for plant-wide industrial processes. *Chemometr. Intell. Lab. Syst.* **2017**, *171*, 16–25. [CrossRef]
18. Qin, S.J. Survey on data-driven industrial process monitoring and diagnosis. *Annu. Rev. Contr.* **2012**, *36*, 220–234. [CrossRef]
19. Russell, E.L.; Chiang, L.H.; Braatz, R.D. Fault detection in industrial processes using canonical variate analysis and dynamic principal component analysis. *Intell. Lab. Syst.* **2000**, *51*, 81–93. [CrossRef]
20. Yoon, S.; MacGregor, J.F. Statistical and causal model-based approaches to fault detection and isolation. *AIChE J.* **2000**, *46*, 1813–1824. [CrossRef]
21. Jackson, J.E.A. *User's Guide to Principal Component, New York*; Wiley-Inter-Science: Hoboken, NJ, USA, 1991.
22. Chiang, L.H.; Russell, E.L.; Braatz, R.D. *Fault Detection and Diagnosis in Industrial Systems*; Springer Science & Business Media: Medford, MA, USA, 2000.
23. Sheriff, M.Z.; Botre, C.; Mansouri, M.; Nounou, H.; Nounou, M.; Karim, M.N. Process monitoring using data-based fault detection techniques: Comparative studies. In *Fault Diagnosis and Detection*; InTechOpen Science: London, UK; pp. 237–261.
24. Lee, J.M.; Yoo, C.; Choi, S.W.; Vanrolleghem, P.A.; Lee, I.B. Nonlinear process monitoring using kernel principal component analysis. *Chem. Eng. Sci.* **2004**, *59*, 223–234. [CrossRef]
25. Kramer, M.A. Autoassociative neural networks. *Comput. Chem. Eng.* **1992**, *16*, 313–328. [CrossRef]
26. Dong, D.; McAvoy, T.J. Nonlinear principal component analysis—Based on principal curves and neural networks. *Comput. Chem. Eng.* **1996**, *20*, 65–78. [CrossRef]
27. Jia, F.; Martin, E.B.; Morris, A.J. Non-linear principal components analysis with application to process fault detection. *Int. J. Syst. Sci.* **2000**, *31*, 1473–1487. [CrossRef]
28. Cheng, C.; Chiu, M.S. Nonlinear process monitoring using JITL-PCA. *Chemom. Intell. Lab. Syst.* **2005**, *76*, 1–13. [CrossRef]
29. Kruger, U.; Antory, D.; Hahn, J.; Irwin, G.W.; McCullough, G. Introduction of a nonlinearity measure for principal component models. *Comput. Chem. Eng.* **2005**, *29*, 2355–2362. [CrossRef]
30. Scholkopf, B.; Smola, A.; Muller, K.-R. Nonlinear component analysis as a kernel eigenvalue problem. *Neural Comput.* **1998**, *10*, 1299–1319. [CrossRef]
31. Cristianini, N.; Shawe-Taylor, J. *An Introduction to Support Vector Machines and Other Kernel-Based Learning Methods*; Cambridge University Press: New York, NY, USA, 2000.
32. Schölkopf, B.; Smola, A.; Müller, K.R. Kernel principal component analysis. In *International Conference on Artificial Neural Networks*; Springer: Berlin, Germany, 1997; pp. 583–588.
33. Choi, S.W.; Lee, C.; Lee, J.M.; Park, J.H.; Lee, I.B. Fault detection and identification of non-linear processes based on kernel PCA. *Chemom. Intell. Lab. Syst.* **2005**, *75*, 55–67. [CrossRef]
34. Sheriff, M.Z.; Karim, M.N.; Nounou, H.N.; Nounou, M.N. Process monitoring using PCA-based GLR methods: A comparative study. *J. Comput. Sci.* **2018**, *27*, 227–246. [CrossRef]
35. Hoffmann, H. Kernel PCA for novelty detection. *Pattern Recognit.* **2007**, *40*, 863–874. [CrossRef]
36. Fan, Y.; Wang, H.; Zhao, X.; Yang, Q.; Liang, Y. Short-Term Load Forecasting of Distributed Energy System Based on Kernel Principal Component Analysis and KELM Optimized by Fireworks Algorithm. *Appl. Sci.* **2021**, *11*, 12014. [CrossRef]
37. Zhu, M.; Ghodsi, A. Automatic dimensionality selection from the scree plot via the use of profile likelihood. *Comput. Stat. Data Anal.* **2006**, *51*, 918–930. [CrossRef]
38. Jolliffe, I. *Principal Component Analysis*, 2nd ed.; Springer: Berlin, Germany, 2002.
39. Bowman, A.W.; Azzalini, A. *Applied Smoothing Techniques for Data Analysis: The Kernel Approach With S-Plus Illustrations*; OUP Oxford: Berlin, Germany, 1997; Volume 18.
40. Sheriff, M.Z.; Basha, N.; Karim, M.N.; Nounou, H.; Nounou, M. Fault Detection of Single and Interval Valued Data Using Statistical Process Monitoring Techniques. In *Fault Detection, Diagnosis and Prognosis*; IntechOpen: London, UK, 2019. [CrossRef]
41. Alcala, C.F.; Joe Qin, S. Analysis and generalization of fault diagnosis methods for process monitoring. *J. Process Control.* **2011**, *21*, 322–330. [CrossRef]
42. Khusna, H.; Mashuri, M.; Ahsan, M.; Suhartono, S.; Prastyo, D.D. Bootstrap Based Maximum Multivariate CUSUM Control Chart. *Qual. Technol. Quant. Manag.* **2018**, *17*, 52–74. [CrossRef]